DOI: 10.19884/j.1672-5220.202309006

Comparative Study on Chitosan Modified with Different Hepatocyte Ligands as Scaffold Material for Liver Tissue Regeneration: Preparation, Characterization and Evaluation

WANG Zhe[1], YU Fan[1], JIANG Yuxin[2], HOU Yuting[1], SHUAI Lan[1], DENG Min[2*], WANG Hongsheng[1*]
1. Shanghai Engineering Research Center of Nano-Biomaterials and Regenerative Medicine, College of Biological Science and Medical Engineering, Donghua University, Shanghai 201620, China
2. The Affiliated Hospital of Jiaxing University, Jiaxing Key Laboratory of Virus-Related Infectious Diseases, Jiaxing University, Jiaxing 314001, China

Abstract: To achieve the ideal scaffolds for liver tissue regeneration, chitosan (CS) was modified with lactobionic acid (LA) or/and glycyrrhetinic acid (GA) to obtain LA-modified CS (LC), GA-modified CS (GC) and GA/LA-modified CS (GLC), and the composite nanofibrous scaffolds composed of silk fibroin (SF) and the above modified CS were fabricated by green electrospinning. Fourier transform infrared (FTIR) spectroscopy, nuclear magnetic resonance (NMR) spectroscopy and X-ray diffraction (XRD) patterns were used to characterize the chemical components and structures. The water contact angle was measured to evaluate the hydrophilicity, and thermal gravimetric analysis (TGA) was carried out to obtain the thermal properties. These scaffolds were hydrophilic, and their hydrophilicity and thermal stability decreased with the increase of the modified CS content, while their crystallinity increased. The scaffolds showed good performance in promoting the proliferation of the human hepatoma cell line (HepG2 cell) as well as their secretion of both albumin and urea. Furthermore, the scaffolds with LC had a better performance of hepatocellular compatibility than those with GC or GLC.

Key words: glycyrrhetinic acid (GA); galactose; chitosan (CS); silk fibroin (SF); liver tissue engineering
CLC number: R9 **Document code**: A
Article ID: 1672-5220(2024)03-0263-12

Open Science Identity (OSID)

0 Introduction

Severe liver diseases such as liver failure, cirrhosis and liver cancer have a poor prognosis, leading to many deaths annually[1]. It is currently recognized that the most effective treatment is liver transplantation, but due to the shortage of donors, high costs and related complications, its practicality is limited[2]. Meanwhile, hepatocyte loses its biological activity quickly, making it hard for hepatocyte transplantation[3]. The development of tissue engineering has brought a new solution to liver transplantation, which is expected to alleviate the severe shortage of donor organs[4-5]. The ideal scaffolds for liver tissue engineering should have suitable mechanical properties, chemical components and similar structure to the native liver, so as to maintain the viability and function of hepatocytes[6-7].

Galactose is a specific ligand for the asialoglycoprotein receptor (ASGPR) on the surface of liver cells[8-9]. Glycyrrhetinic acid (GA) is the main component of the root of licorice used for hundreds of years as a traditional Chinese drug[10-11]. There are plenty of GA receptors on the liver cell membrane, making it easy to enrich or aggregate in the human liver[12-13]. Chitosan (CS) nanoparticles modified with galactose or GA have been reported to have the ability to target liver cells[14-15]. As a unique alkaline polysaccharide, CS has good biocompatibility, mechanical properties, antibacterial properties and blood coagulation promotion function[16-17]. Besides, the pyran ring in the molecular structure of CS has active groups such as amino and hydroxyl groups[18], which is convenient for grafting different chemical groups to achieve corresponding functions. The carboxyl group of lactobionic acid (LA) or GA can react with the amino group of CS under corresponding conditions to synthesize LA-modified CS (LC)[9], GA-modified CS (GC)[19] and GA/LA-modified CS (GLC)[20-21]. These kinds of modified CSs are expected to promote the adhesion and proliferation of liver cells. We previously reported the nanofibrous scaffolds composed of silk fibroin (SF) and galactosylated CS with a good performance in promoting

Received date: 2023-09-25
Foundation items: Science & Technology Commission of Shanghai Municipality (No. 20DZ2254900); Municipal Public Welfare Research Project from Jiaxing, Zhejiang Province (No. 2022AY10001); Open Project Program of Jiaxing Key Laboratory of Virus-Related Infectious Diseases.
* Correspondence should be addressed to WANG Hongsheng, email: whs@dhu.edu.cn; DENG Min, email: 00135084@zjxu.edu.cn
Citation: WANG Z, YU F, JIANG Y X, et al. Comparative study on chitosan modified with different hepatocyte ligands as scaffold material for liver tissue regeneration: preparation, characterization and evaluation [J]. *Journal of Donghua University (English Edition)*, 2024, 41(3): 263-274.

the proliferation of hepatocytes[22]. So far, there is seldom investigation on hepatocellular compatibility of the scaffolds containing GC. And it is meaningful to compare the effects of LC and/or GC as part of the scaffolds on hepatocytes' growth and function, which helps to find more ideal strategies for constructing liver tissue engineering scaffolds.

Electrospinning has emerged as a promising technology to construct nanofibrous scaffolds[23]. The electrospun composite nanofibers composed of proteins and polysaccharides can mimic the structure of the natural extracellular matrix (ECM), which promotes cell adhesion, proliferation and differentiation[18,24-25]. SF is a polymer extracted from natural mulberry silk after degumming treatment, which has excellent biocompatibility and biodegradability[6,26-27]. Though the electrospun pure SF is brittle, the electrospun SF/CS composite nanofibers have much better mechanical properties. Moreover, the electrospun SF/CS composite nanofibrous scaffolds are similar in composition and structure to the natural ECM. Therefore, the combination of SF and GC, LC, or GLC could be a good choice for constructing electrospun scaffolds for liver tissue regeneration.

Based on the above understanding, we aim to develop a novel liver regeneration scaffold with SF and LC or/and GC by green electrospinning without involving toxic and harmful substances, and explore the performance of these scaffolds containing different ligands for hepatocytes. The physical and chemical properties of the modified CS as well as the electrospun composite nanofibrous scaffolds are characterized. The as-spun scaffolds are also evaluated for their biosafety and hepatocellular compatibility by in vitro assays.

1 Materials and Methods

1.1 Materials

Anhydrous sodium carbonate (Na_2CO_3), dimethyl sulfoxide (DMSO) and dimethylformamide (DMF) were purchased from Sinopharm Chemical Reagent Co., Ltd., China. *N*-hydroxysuccinimide (NHS) and 1-ethyl-3 (3-dimethylamino) carbodiimide hydrochloride (EDC·HCl) were purchased from Shanghai Demer Pharmaceutical Technology Co., Ltd., China. A dialysis bag with a molecular weight cutoff value (MWCV) of 14 000 was sourced from Beijing Jingke Hongda Biotechnology Co., Ltd., China. Tetramethylethylenediamine (TEMED) and LA were obtained from Shenggong Bioengineering Co., Ltd., China. CS and GA were purchased from Shanghai Bangcheng Chemical Co., Ltd., China. Glacial acetic acid (HAc) was purchased from Shanghai Lingfeng Chemical Reagent Co., Ltd., China. Lithium bromide (LiBr) was obtained from Shanghai Demer Technology Co., Ltd., China. The above chemical reagents were analytical grade. Silk cocoon shells were purchased from Zhejiang Jiaxing Silk Co., Ltd., China. Fetal bovine serum (FBS) and 3-(4, 5-dimethylthiazol-2-yl)-2, 5-diphenyltetrazolium bromide (MTT) were purchased from Huamei Bioengineering Company, China. The enzyme-linked immunosorbent assays (ELISA) kits were purchased from Beyotime Biotech. Inc., China. Paraformaldehyde was purchased from Wuhan Servicebio Technology Co., Ltd., China. Dulbecco's minimum essential medium (DMEM) and minimum essential medium (MEM) were purchased from Shanghai Yapei Biotechnology Co., Ltd., China. Mouse fibroblast cell line (L929 cell) and human hepatoma cell line (HepG2 cell) were provided by the Institute of Biochemistry and Cell Biology (Chinese Academy of Sciences, China). Calcitonin-am/propidium iodide (PI) double staining kit was purchased from Yeasen Biotechnology (Shanghai) Co., Ltd., China. Other routine chemicals were purchased from Sinopharm Chemical Reagent Co., Ltd., China.

1.2 Methods

1.2.1 Synthesis of LC, GC and GLC

LC was synthesized according to the previous study[9]. Briefly, 2.0 g LA was dissolved in 50 mL TEMED/HCl buffer solution. Then 0.6 g EDC · HCl and 0.14 g NHS were added to the solution and stirred for 30 min to activate the carboxyl group. Subsequently, 1.0 g CS was dissolved in an acetic acid solution with a volume fraction of 0.5%, and the pH was adjusted to 5.5 with 0.1 mol/L NaOH before being added to the LA solution. Then, the reactants reacted at room temperature for 3 d. After filtration, the reaction solution was dialyzed in distilled water for 3 d by changing water 4 times a day. Finally, LC was obtained after freeze-drying for 3 d and stored at −20 ℃.

GC was synthesized according to the previous study[19]. Firstly, 1.0 g GA was dissolved in 50 mL DMF, then 0.5 g EDC · HCl and 0.3 g NHS were added and stirred for 30 min. Then 0.36 g CS was dissolved in the acetic acid solution (its volume fraction is 0.5%), mixed with GA solution, and reacted at room temperature for one day. Next, the solution was treated with acetone (their volume ratio is 1∶4) and left for 1 d. Finally, the precipitate was washed with ether and ethanol and then put in a vacuum-drying oven for 3 d to obtain GC.

The synthesis of GLC was based on the galactosylation reaction of GC[21]. Firstly, 2.0 g LA was dissolved in 50 mL TEMED/HCL buffer. Then 0.6 g EDC · HCl and 0.14 g NHS were added to the solution and stirred for 30 min. Next, 1.0 g GC was dissolved in the acetic acid solution (its volume fraction is 0.5%), then added to the LA solution and kept stirring at room temperature for 3 d. After filtration, the reaction solution was dialyzed in distilled water for 3 d with the water being changed 4 times a day. Finally, GLC was obtained after freeze-drying and stored at −20 ℃.

Fourier transform infrared (FTIR) spectroscopy and nuclear magnetic resonance (NMR) spectroscopy were

employed to trace the functional groups and confirm the chemical modification. For FTIR analysis, all the samples were scanned in the a wavenumber range of 500 to 4 000 cm^{-1} (Nicolet 6700, Thermo Fisher Scientific, USA). For NMR analysis, an NMR spectrometer (AVANCE400, Bruker, Switzerland) was used. The chemical shift multiplied by 10^6 is denoted by δ in this paper. For elemental analysis, an elemental analyzer (VarioEL III, Elementar, Germany) was used to trace LC, GC and GLC. In addition, the degree of substitution (DS) was determined by elemental analysis according to the previous study[28].

1.2.2 Preparation of composite nanofibrous scaffolds

The extract of SF was processed according to the previous study[6]. Firstly, silkworm cocoon shells were degummed by boiling in Na_2CO_3 solution (a mass fraction of 0.5%) for 30 min and the process was repeated twice. Then, the samples were dried in a 60 ℃ oven after being rinsed with water 5 times. Subsequently, the dried sample (10 g) was immersed in 100 mL LiBr solution (9 mol/L) and was kept reacting at 40 ℃ until dissolved completely. After filtration, the solution was dialyzed in distilled water for 3 d with the water being changed 4 times a day. Finally, after freeze-dried for 3 d, the SF was obtained and stored in a vacuum dryer for further use.

The composite nanofibrous scaffolds were prepared by electrospinning as illustrated in Fig. 1. Briefly, a certain quantity of SF, LC, GC and GLC were dissolved in deionized water and stirred overnight to obtain electrospinning solutions. Especially, polyethylene oxide (PEO) was added to improve the electrospinning performance.

The electrospinning solution formulae are shown in Table 1, and the corresponding scaffolds are named SF, SF/LC15, SF/LC30, SF/LC50, SF/GC15, SF/GC30, SF/GC50, SF/GLC15, SF/GLC30 and SF/GLC50, respectively.

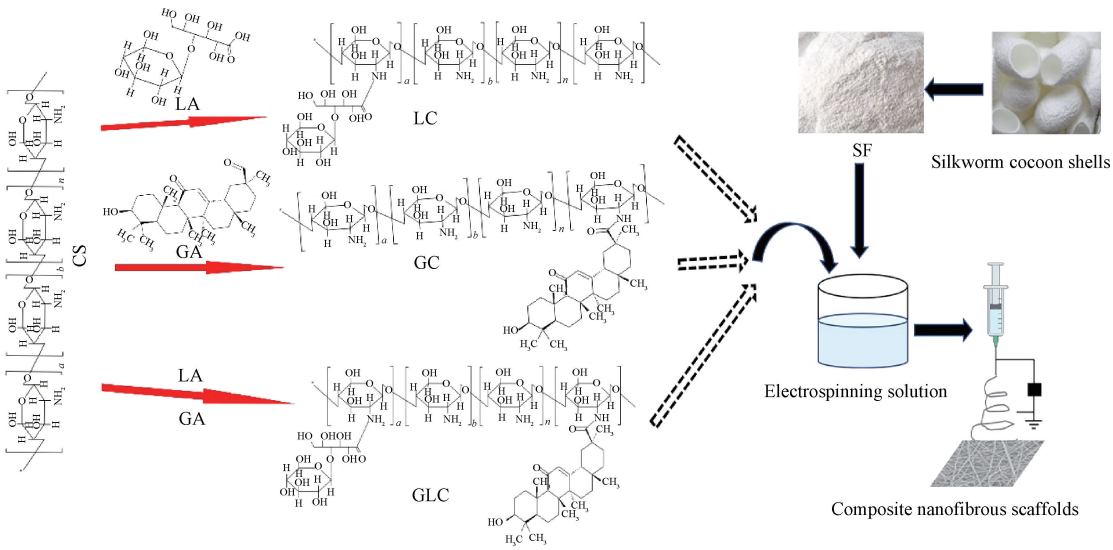

Fig. 1 Schematic illustration of preparation of composite nanofibrous scaffolds

Table 1 Components of electrospinning solution

Group	Modified CS mass/mg			SF	PEO	H_2O
	LC	GC	GLC	mass/g	mass/g	volume/mL
SF	0	0	0	1	0.08	5
SF/LC15	15	0	0	1	0.08	5
SF/LC30	30	0	0	1	0.08	5
SF/LC50	50	0	0	1	0.08	5
SF/GC15	0	15	0	1	0.08	5
SF/GC30	0	30	0	1	0.08	5
SF/GC50	0	50	0	1	0.08	5
SF/GLC15	0	0	15	1	0.08	5
SF/GLC30	0	0	30	1	0.08	5
SF/GLC50	0	0	50	1	0.08	5

The electrospinning solution was treated in an ultrasonic machine for 15 min to remove the bubbles. Then, electrospinning of all samples was done with a 9 gauge needle under the following conditions: voltage of 12 kV, flow rate of 0.8 mL/h and receiving distance of 10 cm. The spinning products were further crosslinked in a container with 75% (volume fraction) ethanol for 10 h. Finally, the composite nanofibrous scaffolds composed of SF and the modified CS were obtained after being put in a vacuum dryer for 2 d to remove residual ethanol.

FTIR was used to investigate the components of the scaffolds. The X-ray diffraction (XRD) pattern was recorded by an X-ray diffractometer (Rigaku MiniFlex 600, Japan) to observe the crystallinity of nanofibers, scanning from 5° to 90° at a scanning rate of 5 (°)/min. The water contact angles (WCAs) of the scaffolds were measured and visualized with an analyzer (OCA40, Dataphysics, Germany) and ImageJ 1.44 software. Thermal gravimetric analysis (TGA) was employed by using a thermogravimetric analyzer (Discovery TGA 550, Waters, USA) to measure the thermal properties of the scaffolds, and the profile was recorded at a heating rate of 10 ℃/min and in a test range of 30 to 900 ℃. The morphologies of the scaffolds were examined by a scanning electron microscope (SEM, Phenom XL, Holland) at 10 kV after the samples were sprayed on 10 nm thick platinum (6 mA, 45 s). The diameters of the nanofibers were determined by the software ImageJ 1.44.

1.2.3 Biocompatibility assays

L929 cells were used to evaluate the cytocompatibility of the scaffolds. Cells were cultured in DMEM containing 10% (volume fraction) FBS and 1% (volume fraction) penicillin/streptomycin. Sterile scaffolds were pressed by steel rings to the bottom of the 24 well plates. The cells were then seeded at a density of 5×10^4 cells/well on the scaffolds and incubated at 37 ℃ with 5% (volume fraction) CO_2. The proliferation of cells on the scaffolds was determined by MTT assay. SEM images were taken to observe cell morphology after the sample was fixed with paraformaldehyde solution (a volume fraction of 4%) for 4 h followed by dehydration and freeze-drying for 3 d.

HepG2 cells were selected to evaluate the hepatocellular compatibility of the scaffolds. The culture of HepG2 cells was the same as L929 cells except that MEM replaced the DMEM. MTT assay was also employed to assess the cell viability. Besides, Live/dead staining was used to observe HepG2 cells on day 1, day 3 and day 5. Furthermore, urea and albumin secreted by HepG2 cells were determined by ELISA kits according to the manufacturer's instructions.

1.2.4 Statistical analysis

All the quantitative data were expressed as mean ± standard deviation (SD). The statistical analysis was carried out using one-way ANOVA, and the result with p-value less than 0.05 was considered statistically significant.

2 Results and Discussion

2.1 Characterization of LC, GC and GLC

The structure changes of CS caused by amidation were confirmed by FTIR spectroscopy (Fig. 2). For LC, the reaction between the carboxyl group from LA and the amine group from CS led to an amide linkage. The peaks at 3 356 cm^{-1} and 3 350 cm^{-1} are the —OH absorption peaks for CS and LC, respectively. The narrow peak at 1 738 cm^{-1} belongs to the carboxyl group from LA. The peaks at 2 918 cm^{-1} and 2 882 cm^{-1} belong to the primary amine bond in CS, while these peaks weaken in LC, indicating that primary amines reacted with the carboxyl group. In addition, the peak at 1 600 cm^{-1} (CS) shifts slightly to 1 642 cm^{-1} (LC), indicating that $—NH_2$ has reacted with —COOH. These results are consistent with previous reports[9,29]. The narrow peak at 1 706 cm^{-1} belongs to the C═O on the carboxyl group of GA. The small peak at 2 877 cm^{-1} in the GC spectrum indicates that the primary amine group from CS has reacted with the carboxyl group from GA. The peak at 1 600 cm^{-1} disappears in the GC spectrum, while new peaks appear at 1 560 cm^{-1} and 1 654 cm^{-1}. These results are in agreement with the previous study[19], indicating that CS has reacted with GA successfully. For GLC, the peak at 1 738 cm^{-1} (LA) disappears, which belongs to the C═O group. In contrast, the peak of the ester bond appears at 1 742 cm^{-1}. The peaks at 1 654 cm^{-1}, 1 560 cm^{-1} and 1 315 cm^{-1} (GC), which belong to amide I, amide II and amide III, shift to 1 742 cm^{-1}, 1 553 cm^{-1} and 1 319 cm^{-1} (GLC), respectively. These results are in agreement with other studies[20-21], indicating that GC has reacted with LA and that GLC is successfully synthesized.

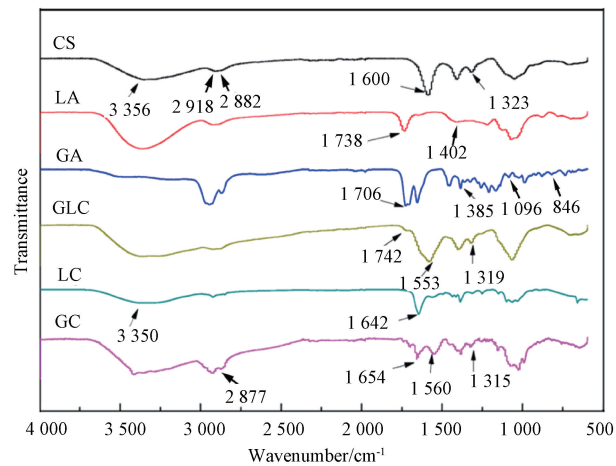

Fig. 2 FTIR characterization of CS, LA, GA and the modified CS (LC, GC and GLC)

It is worth noting that the acylation activity of the carboxyl group is weak, and the partly deacylated CS has a sizeable steric hindrance[13], making it difficult

to graft multiple ligands to CS. Therefore, to improve the grafting rate, we chose EDC · HCl and NHS as the activator and protective agent to act on the carboxyl group and primary amine. CS first reacted with GA to obtain GC, and then GC reacted with LA to obtain GLC. This sequential reaction resulted in higher efficiency due to the reduction of the steric hindrance.

As shown in Fig. 3, a new peak at δ = 4.3 in the spectrum of LC belongs to the protons in the methylene attached to hydroxy 4 group (—CH(OH)—) (▲) from LA. The peak at δ = 1.9 in the LC spectrum refers to the sugar protons from LA, indicating that the galactose residues are grafted on the CS backbone and that LC is synthesized successfully. There is a new peak at δ = 1.0 in the spectrum of GC, which refers to methyl and methylene protons (★) from GA and indicates that GA is grafted on the CS backbone, i. e. GC is synthesized successfully. Also, new peaks at δ = 2.7 and 4.2 in the GLC spectrum refer to the methyl protons from GA (★) and methylene protons (▲) from LA, respectively, indicating that both the GA and galactose groups are grafted on the CS amino group, i. e. GLC is synthesized successfully.

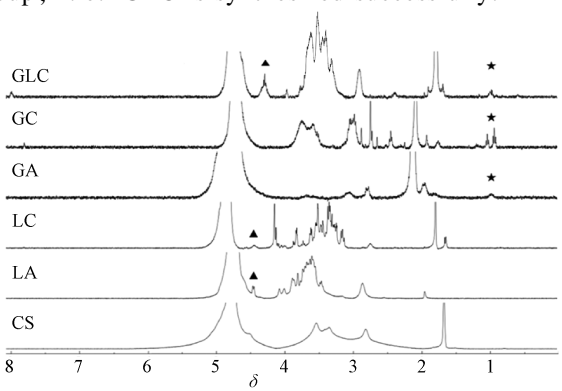

Fig. 3 ^{1}H NMR characterization

The element composition of the modified CS was measured by an elemental analysis test. As shown in Table 2, the element mass fractions of C, H and N are slightly changed after the amidation reaction. By calculating the amino reaction rate, the DS of LC, GC and GLC is 51.9%, 1.9% and 27.4%, respectively. The multi-ring structure of GA leads to a molecule with rigidity and steric hindrance, which is not conducive to the substitution reaction on the CS molecule. Therefore, the DS of GLC and GC are much lower than that of LC.

Table 2 Elemental analysis data

Sample	Mass fraction/%			DS/%
	C	H	N	
CS	39.06	6.89	7.22	—
LC	36.79	6.74	3.42	51.9
GC	39.58	6.97	6.71	1.9
GLC	38.31	6.92	4.74	27.4

2.2 Characterization of composite nanofibrous scaffolds

As shown in Fig. 4, the electrospun composite nanofibers are circular, with uniform diameter distribution and smooth surfaces. The average diameter of SF/LC slightly increases with the increase of LC, while that of SF/GC and SF/GLC slightly decreases with the increase of GC or GLC content. The diameter of electrospun fibers can be influenced by the surface tension of the electrospinning solution, which depends on the viscosity of the solution[30-31]. Usually, the higher the viscosity of the solution, the greater its surface tension, and the larger the diameter of the fibers produced[32-34]. LC has good water solubility, and its addition increases the viscosity of the electrospinning solution, which should be responsible for the increase in diameter of the SF/LC fibers. Smaller diameters at higher GC or GLC content could be due to the rigid chemical structure of GA which reduced the viscosity of SF electrospinning solution and thereby resulted in a corresponding reduction in the diameter of the fibers.

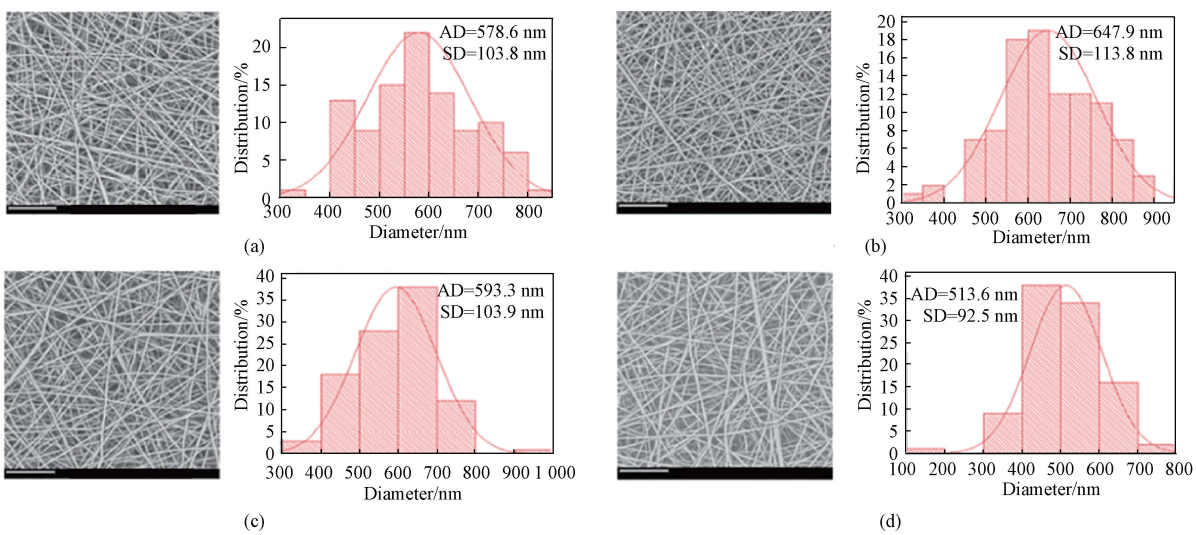

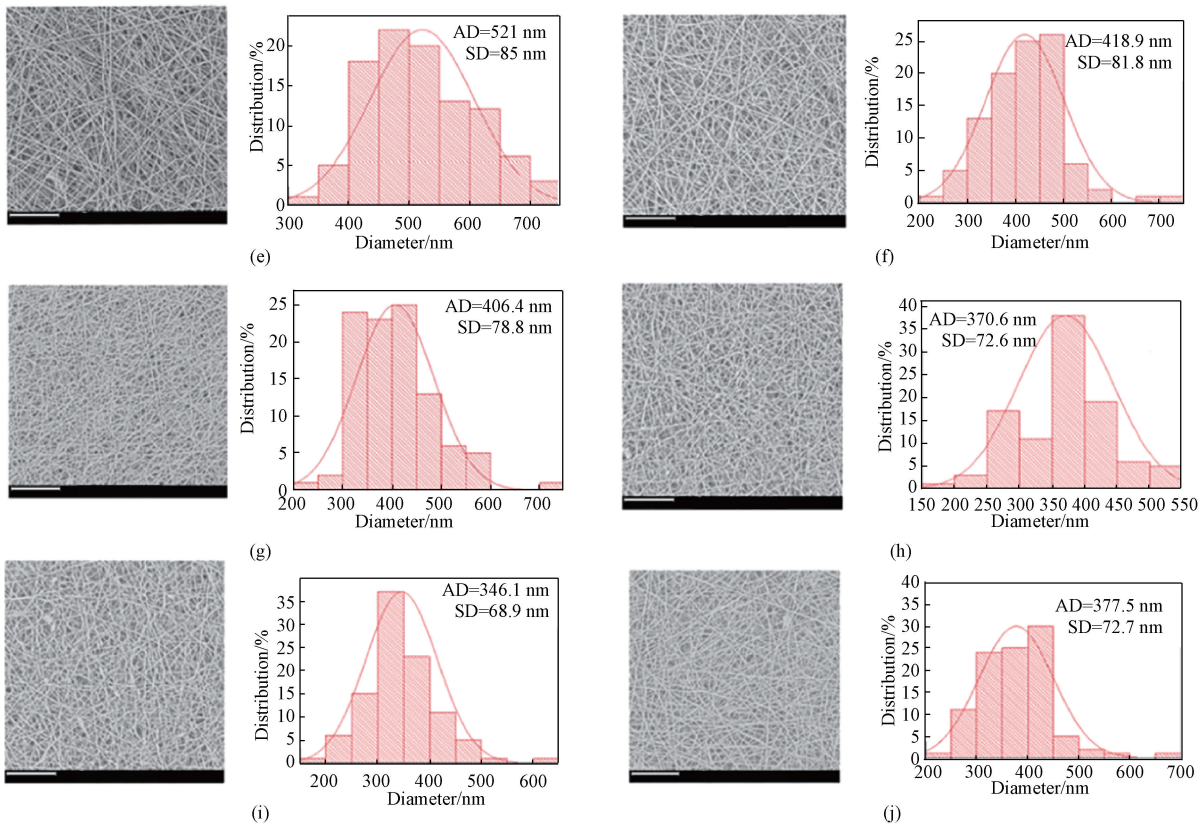

Fig. 4 SEM images and diameter distributions of the SF, SF/LC, SF/GC and SF/GLC nanofibers (scale bar is 30 μm; AD means average diameter): (a) SF; (b) SF/LC15; (c) SF/LC30; (d) SF/LC50; (e) SF/GC15; (f) SF/GC30; (g) SF/GC50; (h) SF/GLC15; (i) SF/GLC30; (j) SF/GLC50

These scaffolds were also measured by FTIR and XRD. As shown in Fig. 5 (a), SF has specific amide peaks at 1 650–1 660 cm^{-1} (amide I), 1 535–1 545 cm^{-1} (amide II) and 1 235–1 240 cm^{-1} (amide III)[35]. After the crosslinking process, the absorption peaks shift to 1 625 – 1 640, 1 515 – 1 525 and 1 265 cm^{-1}, respectively, representing the β-sheet in SF. The characteristic peaks (2 940, 1 167 and 1 081 cm^{-1}) of LC appear in SF/LC, and the characteristic peaks (2 937, 1 381, 1 170 and 1 078 cm^{-1}) of GC appear in SF/GC, indicating that LC or GC combined with SF successfully. The absorption peaks of SF/GLC appear at 2 878 cm^{-1} and 1 456 cm^{-1}, and the characteristic peaks of LA and GA at 1 402, 1 096 and 846 cm^{-1} also appear. These results show that LC, GC and GLC are successfully crosslinked with SF. The 2θ angles of SF/LC, SF/GC and SF/GLC have a strong diffraction peak near 22° (Figs. 5(b)–5(d)). The crystallization of SF/LC15, SF/LC30 and SF/LC50 are 17.53%, 19.32% and 22.36%, respectively, larger than that of pure SF (16.61%). The crystallization of SF/GC15, SF/GC30 and SF/GC50 are 17.96%, 20.03% and 20.57%, respectively. The crystallization of SF/GLC15, SF/GLC30 and SF/GLC50 are 19.23%, 22.32% and 25.94%, respectively. These results indicate that the crystallization of the composite nanofibrous scaffolds rises with the increase of the modified CS content. No significant difference in crystallinity is observed among SF/LC, SF/GC and SF/GLC. The increase in crystallinity is beneficial to the mechanical properties and chemical resistance of the scaffolds, which is useful for clinical use[30-31].

TGA analysis was employed to measure thermal stability and decomposition. As shown in Fig. 6, during the heating process from 30 ℃ to 900 ℃, the mass loss can be divided into three stages. In the first stage (30–120 ℃), the mass loss is 10%, caused by the loss of moisture (adsorbed, bounded and crystal water) on nanofibers. In the second stage (120–400 ℃), the mass loss is higher than that in the first stage, accounting for about 40%, due to the thermal degradation, such as the oxidation and decomposition of protein and partial breakdown of the peptide bond (—CO—NH—). In the third stage (400–900 ℃), the mass loss is about 10%, mainly due to the breakdown of the polypeptide chain and the modified CS, which could be ascribed to the disruption of —CO—NH—, C—C, C—O and N—N covalent bonds. The residual mass percentage of nanofibers is about 38%. Compared with the pure SF nanofibers, the thermal stability of the composite nanofibers decreased, which could be due to the weakened molecular interaction in the composites.

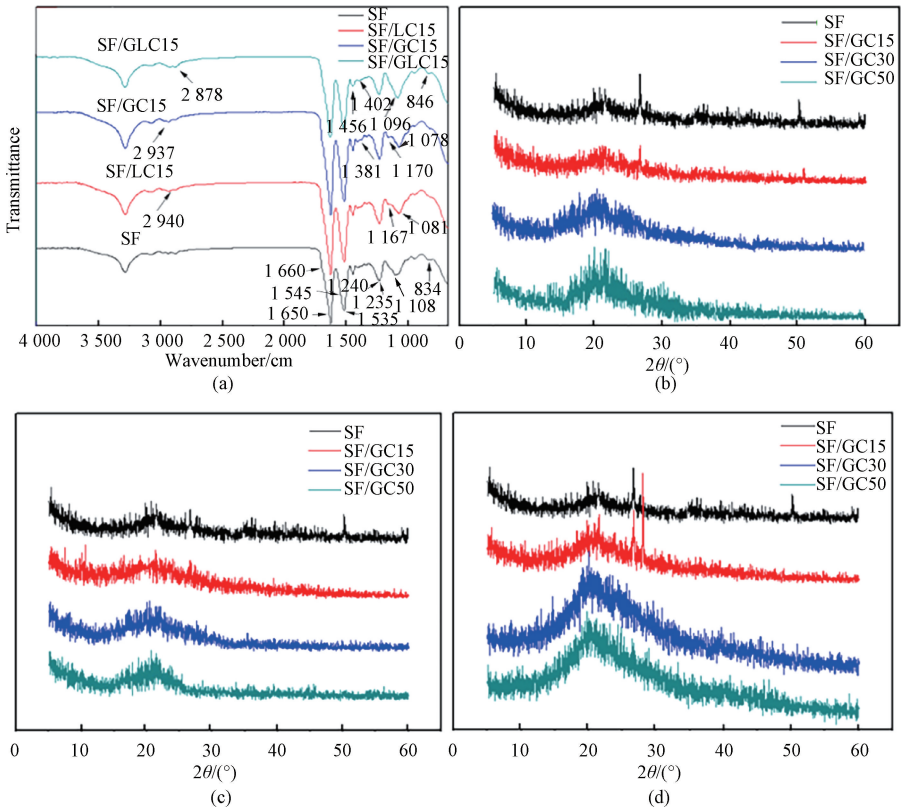

Fig. 5 FTIR spectra and XRD patterns of scaffolds: (a) FTIR spectra of SF/LC, SF/GC and SF/GLC; (b) XRD patterns of SF/LC; (c) XRD patterns of SF/GC; (d) XRD patterns of SF/GLC

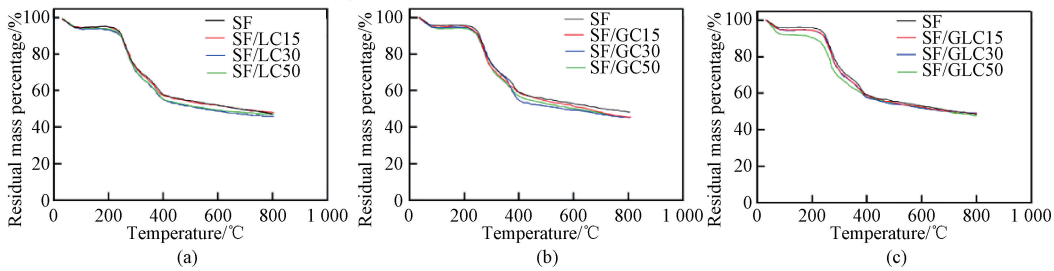

Fig. 6 TGA of composite nanofibrous scaffolds: (a) SF/LC; (b) SF/GC; (c) SF/GLC)

The hydrophilicity of these scaffolds is vital for cell adhesion and proliferation. Here, the hydrophilicity of the composite nanofibrous scaffolds was assessed by measuring the WCA. As shown in Fig. 7, the WCA of SF is 0°, while that of the composite nanofibrous scaffolds increases due to the addition of the modified CS. The higher the modified CS content, the lower the hydrophilicity of the composite nanofibrous scaffold. Among the three modified CS, the addition of GC has the greatest impact on the hydrophilicity of SF, followed by GLC. The composite nanofibrous scaffolds have good hydrophilicity as their WCAs are less than 90°, which should ascribed to the hydrophilicity of SF and the abundance of the hydroxyl group on CS[36]. The hydrophilic properties of these scaffolds are beneficial to cell adhesion and proliferation.

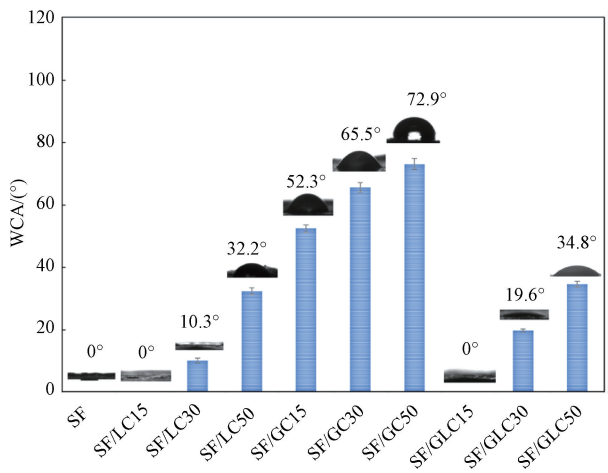

Fig. 7 WCA of scaffolds

2.3 Cytocompatibility of composite nanofibrous scaffolds

The cytocompatibility of the composite nanofibrous scaffolds was evaluated by investigating the viability of L929 cells cultured on these scaffolds. As shown in Fig. 8(a), these scaffolds significantly enhance the proliferation of L929 cells, and the composite nanofibrous scaffolds with more modified CS show better performance. Furthermore, SF/LC50 show the best performance in promoting cell proliferation. The morphology of L929 cells cultured on the composite nanofibrous scaffolds was also observed by SEM. As shown in Fig. 8 (b), the cells exhibit good spreading morphology on the composite nanofibrous scaffolds. These results indicate that the composite nanofibrous scaffolds, especially SF/LC50, have good cytocompatibility, which is due to their chemical components, high porosity, specific surface area and good hydrophilicity[37].

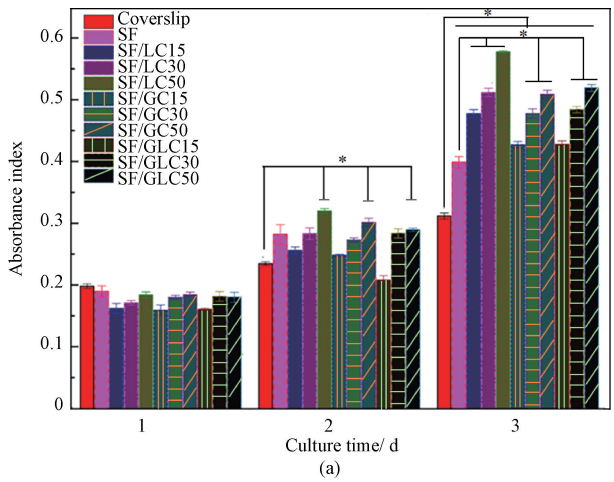

Fig. 8 L929 cells cultured on composite nanofibrous scaffolds: (a) viabilities (* means $p<0.05$); (b) SEM images (the scale bar is 30 μm)

2.4 Hepatocellular compatibility of composite nanofibrous scaffolds

The hepatocellular compatibility of the composite nanofibrous scaffolds was assessed by investigating the viability and expression of landmark functional proteins of HepG2 cells cultured on these scaffolds. As shown in Fig. 9, compared with the scaffold made of pure SF, there are more cells on the composite nanofibrous scaffolds with the modified CS, and the cells cultured on SF/LC50 show the best viability. SEM images in Fig. 9(b) show that the cells cultured on the scaffolds are in good condition, with some growing into the nanofibers and exhibiting good interactions with the scaffold. Compared with the pure SF scaffold, the composite nanofibrous scaffolds significantly enhanced cell proliferation, which might be related to the presence of the modified CS that could be specifically recognized by hepatocytes. These results indicate that the composite nanofibrous scaffolds, particularly SF/LC50, can promote the proliferation of hepatocytes.

Albumin is a molecule secreted by hepatocytes and can modulate important physiological processes, such as the transmission of molecular and regulation of colloidal osmotic pressure[38]. Albumin and urea are hepatocyte-specific molecules and are necessary for liver function[39]. HepG2 cells are similar to normal hepatocytes in secretion of urea and albumin[40]. The expression of albumin and urea was measured by ELISA according to the standard curves obtained by instructions. As shown in Fig. 10, SF/LC50 and SF/GLC50 significantly improve the secretion levels of urea compared with the pure SF. The level of albumin induced by SF/LC50 is also higher than that of pure SF. These results indicate that the scaffolds containing LC or GLC are beneficial to the expression of functional genes in hepatocytes. Meanwhile, SF/LC50 induces higher secretion levels of urea and albumin than SF/GLC50 and SF/GC50 because LC has much higher DS and hydrophilicity than GC. Due to the much higher DS of LC compared to GC or GLC (Table 2), LC can be a more suitable material for constructing liver tissue regeneration scaffolds as demonstrated by the above data. Given the superior properties, including natural sources, components and structures resembling natural ECM, good hydrophilicity and biocompatibility, SF/LC50 could be an excellent candidate material with great potential for application in the field of liver tissue regeneration.

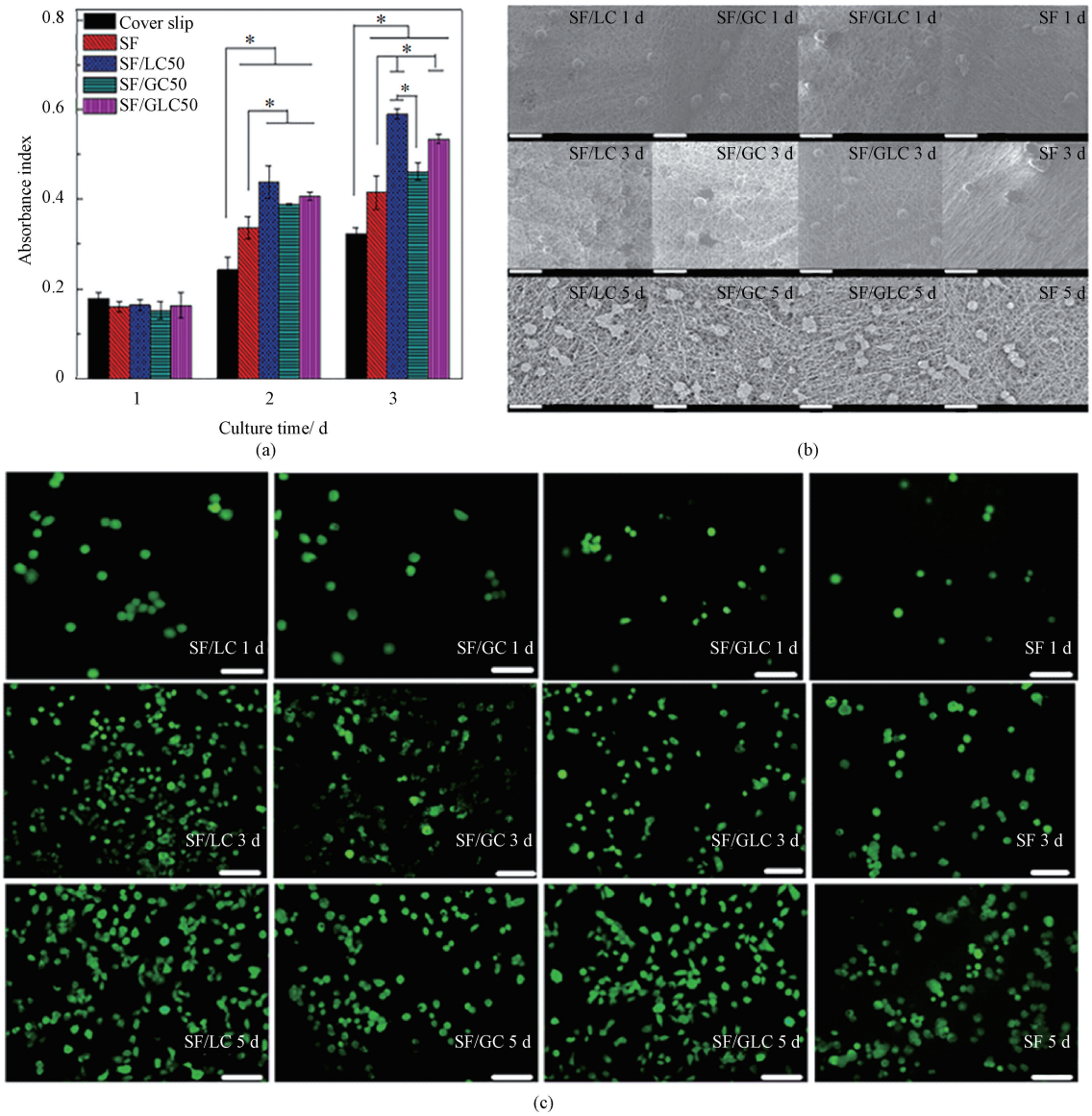

Fig. 9 HepG2 cells cultured on different scaffolds: (a) viabilities (* means $p<0.05$); (b) SEM images (the scale bar is 30 μm); (c) fluorescence micrograph (the scale bar is 30 μm)

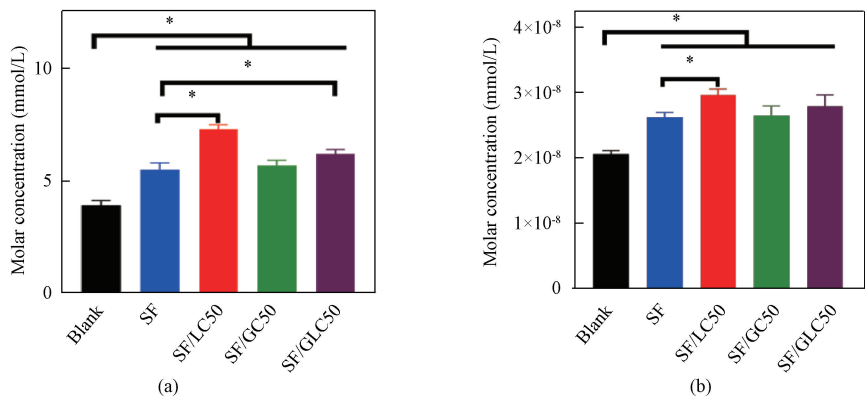

Fig. 10 Levels of secretions in HepG2 cells cultured on different scaffolds: (a) urea; (b) albumin (* means $p<0.05$)

3 Conclusions

In this study, the modified CSs (LC, GC and GLC) were synthesized through the amidation reaction. The nanofibrous scaffolds composed of SF and the modified CS were then fabricated successfully by green electrospinning. The composite nanofibers with smooth surfaces, have a diameter distribution of 350–650 nm. The existence of the modified CS increases the crystallinity of nanofibers and slightly decreases their hydrophilicity and thermal stability. The as-spun composite nanofibrous scaffolds significantly promote the proliferation of HepG2 cells and their secretion of albumin and urea. Furthermore, the composite nanofibrous scaffolds containing more LC have better performance of hepatocellular compatibility than those containing GC or GLC, indicating that LC is a more suitable material for constructing liver tissue regeneration scaffolds. Considering its good hepatocellular compatibility as well as its natural source, SF/LC50 shows promising prospects for liver tissue regeneration.

References

[1] ASRANI S K, DEVARBHAVI H, EATON J, et al. Burden of liver diseases in the world[J]. *Journal of Hepatology*, 2019, 70(1): 151-171.

[2] LINARES I, HAMAR M, SELZNER N, et al. Steatosis in liver transplantation: current limitations and future strategies [J]. *Transplantation*, 2019, 103(1): 78-90.

[3] LEE J S, SHIN J, PARK H M, et al. Liver extracellular matrix providing dual functions of two-dimensional substrate coating and three-dimensional injectable hydrogel platform for liver tissue engineering [J]. *Biomacromolecules*, 2014, 15(1): 206-218.

[4] KULIG K M, VACANTI J P. Hepatic tissue engineering[J]. *Transplant Immunology*, 2004, 12(3/4): 303-310.

[5] OHASHI K, YOKOYAMA T, YAMATO M, et al. Engineering functional two-and three-dimensional liver systems *in vivo* using hepatic tissue sheets[J]. *Nature Medicine*, 2007, 13: 880-885.

[6] KASOJU N, BORA U. Silk fibroin based biomimetic artificial extracellular matrix for hepatic tissue engineering applications [J]. *Biomedical Materials*, 2012, 7(4): 045004.

[7] JIANG W C, CHENG Y H, YEN M H, et al. Cryo-chemical decellularization of the whole liver for mesenchymal stem cells-based functional hepatic tissue engineering [J]. *Biomaterials*, 2014, 35(11): 3607-3617.

[8] LIU H, WANG H, XU Y H, et al. Lactobionic acid-modified dendrimer-entrapped gold nanoparticles for targeted computed tomography imaging of human hepatocellular carcinoma[J]. *ACS Applied Materials & Interfaces*, 2014, 6(9): 6944-6953.

[9] ZHAO R R, LI T, ZHENG G R, et al. Simultaneous inhibition of growth and metastasis of hepatocellular carcinoma by co-delivery of ursolic acid and sorafenib using lactobionic acid modified and pH-sensitive chitosan-conjugated mesoporous silica nanocomplex [J]. *Biomaterials*, 2017, 143: 1-16.

[10] ZHOU N, ZOU C Y, QIN M L, et al. A simple method for evaluation pharmacokinetics of glycyrrhetinic acid and potential drug-drug interaction between herbal ingredients [J]. *Scientific Reports*, 2019, 9: 11308.

[11] HUANG W, WANG W, WANG P, et al. Glycyrrhetinic acid-functionalized degradable micelles as liver-targeted drug carrier [J]. *Journal of Materials Science: Materials in Medicine*, 2011, 22(4): 853-863.

[12] ZHANG C N, WANG W, LIU T, et al. Doxorubicin-loaded glycyrrhetinic acid-modified alginate nanoparticles for liver tumor chemotherapy[J]. *Biomaterials*, 2012, 33(7): 2187-2196.

[13] CAI Y E, XU Y Q, CHAN H F, et al. Glycyrrhetinic acid mediated drug delivery carriers for hepatocellular carcinoma therapy[J]. *Molecular Pharmaceutics*, 2016, 13(3): 699-709.

[14] ALONSO S. Exploiting the bioengineering versatility of lactobionic acid in targeted nanosystems and biomaterials [J]. *Journal of Controlled Release*, 2018, 287: 216-234.

[15] ROHILLA R, GARG T, BARIWAL J, et al. Development, optimization and characterization of glycyrrhetinic acid-chitosan nanoparticles of atorvastatin for liver targeting [J]. *Drug Delivery*, 2016, 23(7): 2290-2297.

[16] AHSAN S M, THOMAS M, REDDY K K, et al. Chitosan as biomaterial in drug delivery and tissue engineering[J]. *International Journal of Biological Macromolecules*, 2018, 110: 97-109.

[17] LEVENGOOD S L, ZHANG M Q. Chitosan-based scaffolds for bone tissue engineering[J]. *Journal of Materials Chemistry B*, 2014, 2(21): 3161-3184.

[18] CROISIER F, JÉRÔME C. Chitosan-based biomaterials for tissue engineering[J]. *European Polymer Journal*, 2013, 49(4): 780-792.

[19] TIAN Q, ZHANG C N, WANG X H, et al. Glycyrrhetinic acid-modified chitosan/poly (ethylene glycol) nanoparticles for liver-targeted delivery [J]. *Biomaterials*, 2010, 31(17): 4748-4756.

[20] LI M, WANG Y, JIANG S, et al. Biodistribution and biocompatibility of glycyrrhetinic acid and galactose-modified chitosan nanoparticles as a novel targeting vehicle for hepatocellular carcinoma[J]. *Nanomedicine*, 2020, 15(2): 145-161.

[21] CHEN H X, LI M, WAN T, et al. Design and synthesis of dual-ligand modified chitosan as a liver targeting vector[J]. *Journal of Materials Science: Materials in Medicine*, 2012, 23(2): 431-441.

[22] YU F, YANG X X, ZHOU X F, et al. Green electrospun silk fibroin/galactose chitosan composite nanofibrous scaffolds for hepatic tissue engineering[J]. *Journal of Donghua University (English Edition)*, 2017, 34(1): 142-146.

[23] MA X X, ZHANG J, HUANG Z Y, et al. Hydrophilic composite polybutylene terephthalate/polyvinyl alcohol membranes prepared by electrospinning [J]. *Journal of Donghua University (English Edition)*, 2022, 39(6): 549-556.

[24] WU T, HUANG C, CHEN J F, et al. Fabrication of multi-layered composite scaffolds by Bi-directional electrospinning method [J]. *Journal of Donghua University (English Edition)*, 2014, 31(5): 625-629.

[25] GAO Z, LIU Y, WANG C, et al. Hippocampal neuron-derived extracellular matrix coated nanofibrous scaffold for neural tissue engineering [J]. *Journal of Donghua University (English Edition)*, 2019, 36(5): 431-436.

[26] HAN H Y, NING H Y, LIU S S, et al. Silk biomaterials with vascularization capacity [J]. *Advanced Functional Materials*, 2016, 26(3): 421-432.

[27] HUANG H Y, TIAN Z F, YI H G, et al. Designing and cloning of the gene sequence encoding silk fibroin amorphous domain [J]. *Journal of Donghua University (English Edition)*, 2012, 29(6): 489-492.

[28] XIAO B, WAN Y, ZHAO M Q, et al. Preparation and characterization of antimicrobial chitosan-*N*-arginine with different degrees of substitution[J]. *Carbohydrate Polymers*, 2011, 83(1): 144-150.

[29] ZHENG D D, DUAN C X, ZHANG D R, et al. Galactosylated chitosan nanoparticles for hepatocyte-targeted delivery of oridonin [J]. *International Journal of Pharmaceutics*, 2012, 436(1/2): 379-386.

[30] VALIZADEH A, MUSSA FARKHANI S. Electrospinning and electrospun nanofibres [J]. *IET Nanobiotechnology*, 2014, 8(2): 83-92.

[31] CHEN Y, LIU Y H, ZHANG P H. Fabrication and performance of electrospinning fiber membrane for bile duct stents [J]. *Journal of Donghua University (Natural Science)*, 2016, 42(6): 800-808. (in Chinese)

[32] DEITZEL J M, KLEINMEYER J, HARRIS D, et al. The effect of processing variables on the morphology of electrospun nanofibers and textiles [J]. *Polymer*, 2001, 42(1): 261-272.

[33] SUBBIAH T, BHAT G S, TOCK R W, et al. Electrospinning of nanofibers [J]. *Journal of Applied Polymer Science*, 2005, 96(2): 557-569.

[34] YI G H, CHENG X Y, GENG M X, et al. Construction of oriented structure in inner surface of small-diameter artificial blood vessels: a review [J]. *Journal of Donghua University (English Edition)*, 2023, 40(2): 149-163.

[35] ZHANG F, ZUO B Q, BAI L. Study on the structure of SF fiber mats electrospun with HFIP and FA and cells behavior [J]. *Journal of Materials Science*, 2009, 44(20): 5682-5687.

[36] TASIC-KOSTOV M, PAVLOVIC D, LUKIC M, et al. Lactobionic acid as antioxidant and moisturizing active in alkyl polyglucoside-based topical emulsions: the colloidal structure, stability and efficacy evaluation[J]. *International Journal of Cosmetic Science*, 2012, 34(5): 424-434.

[37] HOLLISTER S J. Porous scaffold design for tissue engineering[J]. *Nature Materials*, 2005, 4: 518-524.

[38] BIHARI S, BANNARD-SMITH J, BELLOMO R. Albumin as a drug: its biological effects beyond volume expansion[J]. *Critical Care and Resuscitation*, 2020, 22(3): 257-265.

[39] TAN E H, MA F J, GOPINADHAN S, et al. C/EBPα knock-in hepatocytes exhibit increased albumin secretion and urea production[J]. *Cell and Tissue Research*, 2007, 330(3): 427-435.

[40] WILKENING S, STAHL F, BADER A. Comparison of primary human hepatocytes and hepatoma cell line HepG2 with regard to their biotransformation properties [J]. *Drug Metabolism and Disposition: the Biological Fate of Chemicals*, 2003, 31(8): 1035-1042.

不同肝细胞配体修饰的壳聚糖作为肝组织再生支架材料的比较研究：制备、表征和评价

王　哲[1]，余　凡[1]，姜玉新[2]，侯玉婷[1]，帅　兰[1]，邓　敏[2*]，王红声[1*]

1. 东华大学 生物与医学工程学院，上海纳米生物材料与再生医学工程技术研究中心，上海 201620
2. 嘉兴大学附属嘉兴市第一医院，嘉兴市病毒相关传染性病重点实验室，浙江 嘉兴 314001

摘　要：为了获得理想的肝脏再生支架，使用乳酸（lactobionic acid，LA）或/和甘草次酸（glycyrrhetinic acid，GA）对壳聚糖（chitosan，CS）进行改性，得到LA改性的CS（LC）、GA改性的CS（GC）和GA/LA双改性的CS（GLC），并采用绿色静电纺丝法制备了由丝素蛋白（silk fibroin，SF）和上述改性CS组成的复合纳米纤维支架。这些支架是亲水的，其亲水性和热稳定性随着改性CS的增加而降低，而结晶度则相反。这些支架在促进HepG2细胞增殖及分泌白蛋白和尿素方面表现出良好的性能。此外，与SF/GC或SF/GLC支架相比，SF/LC支架具有更好的肝细胞相容性。

关键词：甘草次酸（GA）；半乳糖；壳聚糖（CS）；丝素蛋白（SF）；肝组织工程